



A SINGLE-STAGE LED DRIVER WITH HIGH-PERFORMANCE PRIMARY-SIDE-REGULATED CHARACTERISTIC GUIDE

Dr. S Anitha

Professor, Department of Electrical and Electronics,
R.M.K Engineering College, Thiruvallur dt.

P Hindu kumar, P Kaleesh Kumar, S Ganesh
UG Scholars, Department of Electrical and Electronics Engineering,
R.M.K. Engineering College, Thiruvallur dt.

Abstract—A traditional fly back LED driver is limited by its low performance, which usually does not reach the power factor (PF) and total harmonic distortion needed according to Energy Star or IEC61000-3-2. The control loop of the primary side from the secondary transformer has low reliability and employs more components, which reduces the power density of the system and increases cost. In this brief, based on single-stage single ended primary inductor converter (SEPIC) and fly back converter, a primary-side-regulated LED driver is proposed to improve the performance of the system. Working in DCM, the SEPIC circuit realizes the PF correction naturally. For the fly back converter, the proposed primary-side-regulated method improves the power density and guarantees accurate control of the output current. A 100-W prototype based on SEPIC-fly back was built to verify the analysis and the experimental results coincided with the analysis results satisfactorily.

Index Terms—High performance, LED driver, primary-side-regulated.

I. INTRODUCTION

Compared to traditional lighting sources, such as fluorescent and incandescent lamps, LEDs have their own unique advantages long working life, energy-saving, high illumination intensity, etc. Therefore, LEDs have been used in many applications, such as general lighting, LCD backlight, decorating lights and so on. In order to ensure good performance of LEDs, a highly efficient and reliable LED driver with constant current output is indispensable. In small and medium power applications, the fly back converter is a popular topology because of its simplicity and isolation characteristic [2]. To satisfy the demand of PF and THD

according to IEC 61000-3-2 and Energy Star, a front stage PFC circuit is necessary.

For the PFC cell, there are many converters that can be used as PFC circuits, such as Buck, Boost, Buck-Boost, SEPIC and others. Buck converter is a step-down circuit, which is suitable for low output voltage loads instead of a high step-down ratio transformer [3]. However, it does not work in the whole half-cycle period, which means the PF is not close to unity. As for the Boost converter, it commonly functions as a PFC cell [4], but its step-up characteristic increases the backward voltage stress. In this brief, the SEPIC converter is selected to operate as a power factor corrector. One reason is that the SEPIC converter has two inductors at the input and output ports. The input inductor can cancel the filter components and limit the ripple of input current, which can be determined through the design procedure. Further, when working in DCM, the PFC function can be achieved naturally. The integration of SEPIC and fly back circuits can also satisfy the demands of IEC61000 and Energy Star. Therefore, the SEPIC is a desirable circuit to be used as a PFC cell.

In order to improve the reliability and increase the power density of the system, a primary-side control method is an attractive choice [6]. This brief presents an integrating capacitor method to solve the ringing effect in the auxiliary winding. A differential amplifier is used to improve the detection accuracy for the secondary-side working time, tDIS. In addition, a mirror capacitor is used to obtain a more precise peak current value. Therefore, the output current can be controlled more precisely compared to the traditional primary-side control method reported in [7]. The performance of the system has been verified by experimental results. The single-stage topology based on SEPIC-fly back is shown in Fig. 1. Next, the primary-side-regulated principle is discussed



in Section II. The design of the LED current estimator cell and sample and hold (S&H) cell. Section IV presents the experimental results of the laboratory-made prototype.

II. PRIMARY-SIDE REGULATING

PRINCIPLE AND CHALLENGES:

The single-stage LED driver contains the SEPIC PFC cell and fly-back DC-DC converter cell. As depicted in Fig. 1, the SEPIC cell consists of two inductors L1, L2, two capacitors C1, C2, two diodes D5, D6, and one shared switch Q. As for the fly-back converter cell, it contains a transformer T, a diode D7, and a shared switch Q. The overall structure of the proposed system including the control scheme.

A. SEPIC PFC CELL:

For the SEPIC PFC cell, the voltage $V_{in}(t)$ is the rectification of input voltage $v_{in}(t)$. As shown in (1), V_m is the amplitude of $V_{in}(t)$ and ω is the angular frequency.

$$V_{in}(t) = V_m |\sin(\omega t)|$$

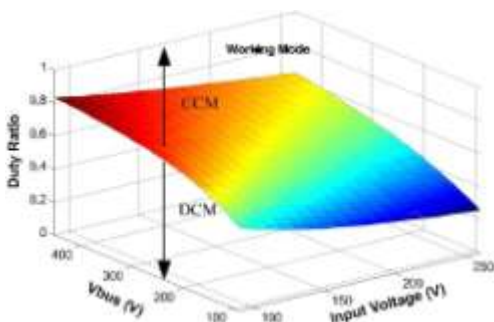
Then, the current i_{L1} through inductor L1 and the current i_{L2} through inductor L2. Here, L1 and L2 are the inductors in the SEPIC circuit and V_{in2} i_0 is the initial value. When $i_{L1} = i_{L2} = i_0$, the current through diode D6 is zero.

Thus, the turn-on time t_{D6} of diode D6 can be calculated. Here, V_{bus} is the voltage of bus capacitor C2, D is the duty ratio and T_s is the switching period. At the same time, the current through diode D6 reaches the peak value. The peak current i_{pD6} of D6. Here, L_{eq} is the equivalent inductor of L1 and L2, where $L_{eq} = L1L2/(L1 + L2)$.

Therefore, the average current of diode D6 in the half switching period.

The average current through the primary inductor L_p is equivalent to the output current of the SEPIC circuit, assuming that the efficiency is 100%; in other words, the input power equals the output power provided to the fly-back circuit. Eq. (6) shows the relationship between P_{in} and P_{fly} .

B. FLYBACK DC-DC CONVERTER CELL:



To ensure that the SEPIC circuit works in DCM, the working mode should satisfy (11) which means that the current through diode D6 is zero during a time interval at the end of the

switching cycle. Here, t_{ON} is the switch turn-on time and t_{OFF} is the time of D6 current changing from peak value to zero when the switch turns off.

$$T_s > t_{ON} + t_{OFF}$$

the DCM or CCM condition. The input voltage is from 90 Vac to 260Vac and V_{bus} ranges from 90V to 450V according to the bus capacitor rated voltage. Below the 3-D surface, the SEPIC circuit works in DCM to result in the PFC function. The CCM working mode operates in the opposite direction.

C. PRIMARY-SIDE-REGULATED CELL:

Next, the LEDs load current will be discussed. The current I_{LED} is the average value of i_{D7} , which is the current of the secondary-side diode D7. When the switch is turned off, the energy in the secondary-side inductor, which comes from the primary inductor L_p , discharges to the LED load. When the current through diode D7 is zero, the primary inductor produces a quasi-resonance with the switch parasitic capacitance. To result in less energy loss, the switch is turned on. The current through the LED, I_{LED} , has the following relationship with current i_{Ls} through diode D7, where T_s is the switching period and i_{Ls} is the current of the secondary inductor.

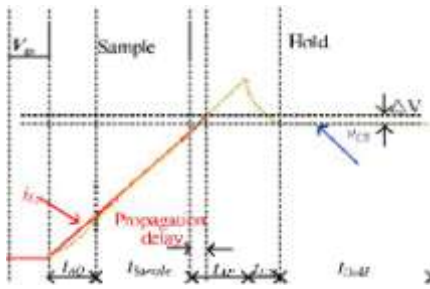
According to the transformer turns ratio n , the relationship between the peak current of the primary inductor i_{Lp} , peak and the current of the secondary inductor i_{Ls} . From (15), in order to accurately get the value of I_{LED} , the detecting components are the peak current i_{Lp} , peak and the discharging time t_{DIS} of the secondary-side diode.

III. ILED ESTIMATOR CELL AND SAMPLE AND HOLD DETECTION CELL

A. TDIS DETECTION CELL DESIGN

According to (15), two elements need to be measured: $i_{Lp,peak}$ and t_{DIS} . The detection circuit of t_{DIS} is proposed. The integrating capacitor C_{aux} is used. To generate a suitable detection signal V_{aux} by filtering the V_{aux} signal of the transformer auxiliary winding. A ripple free measurement voltage V_{aux} can be obtained. The capacitance C_{delay} and the resistance R_{delay} are used to shift the voltage V_{aux} , thus generating the signal delay. Compared with the solution based on a hysteresis comparator, an accurate end instant t_{DIS} can be generated by using a differential amplifier, which outputs the difference between V_{aux} and V_{delay} . The main working principle is explained in next paragraphs.

V_{aux} can quickly reach the valid threshold voltage V_{valid} which can be identified by the zero-crossing comparator. When the voltage V_{aux} changes from negative to positive, the zero-crossing comparator will output a high voltage V_{start} . Then, through the NAND gate, a signal sets the RS trigger to recognize the start instant of t_{DIS} .



The traditional sample-and-hold circuit suffers from one serious drawback: when the circuit is during the holding period, the holding capacitor CH will discharge through the parasitic capacitor Cgd of the switch, rendering an inaccurate value of $i_{Lp,peak}$. This drawback can be overcome by introducing a mirror capacitor CM.

The main working principle is stated as follows and the main waveforms as given.

a) Sample period time: switch SW1 is turned on, while switch SW2 is turned off. The input signal V_{cs} goes through the Buffer to capacitor CH. The Buffer can accelerate the sample speed.

b) Hold period time: switch SW1 is turned off, while switch SW2 is turned on. The charge of capacitor CH discharges to the Gate-Drain capacitor Cgd. Meanwhile, the mirror capacitor C will offset the loss of energy from capacitor CH.

Capacitor CH is located in the feedback loop so it can not be influenced by the output signal. Furthermore, the charge of CH can also be offset by the mirror capacitor CM. Therefore, the hold periods time will present a small error; in other words, the detection peak current $i_{Lp,peak}$ is nearly close to the true value. In addition, it can accelerate the acquisition speed.

IV. EXPERIMENTAL RESULTS

A 100 W single-stage LED driver based on the SEPIC and Flyback converter prototype has the high precision and performance of primary side regulated method. The main characteristics are started as the end instant of Tdis is the moment of the quasi resonant.

(1) Input voltage $V_{in} = 22$

(2) $\sin(100\pi t) = 22$

Start up, so V_{aux} will slowly decline. Shifting V_{aux} , V_{delay} can be obtained. A differential amplifier is used to detect the difference between V_{aux} and V_{delay} . This way as soon as the quasi resonant begins the differential amplifier can output the signal V_{end} better than the hysteresis voltage delay. A comparison between the hysteresis comparator and differential voltage waveforms.

(3) i_{Lp} , PEAK DETECTION CELL DESIGN

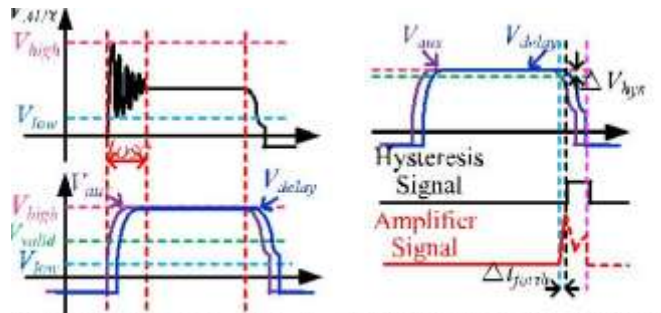
An accurate value of the peak current $i_{Lp, peak}$

(2) input current ripple $I_{rip}/I_{in} = 25\%$

(3) working frequency $F_s = 100\text{KHz}$

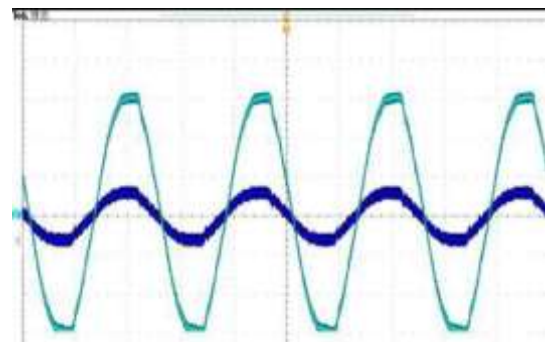
(4) output voltage $V_o = 50\text{ V}$

(5) System efficiency is 90% at the rated 220V output voltage and the input voltage is 111W, where the ripple of the input current is set to be 25% of the input current and the duty ratio is set to be $D = 0.3$. From (9) L_{eq} can be obtained and the inductors can be calculated where $V_{in}(t)$ is $V_m \sin(60)$. $V_{in}(t)$ DTs improved the precision control



(a) The Start Point of t_{rise} Detection (b) The End Point of t_{dis} Detection method.

$$L1 = I_{rip} = 5.01\text{ mH}$$



Input Current and Input Voltage Waveforms.

For the selection of output capacitor C3, the value of capacitor C3 can be selected as per equation (18), where f_{line} is the line frequency and V_o is the ripple of output voltage. The value of C3 is selected to be $68\mu\text{F}$ to decrease the ripple of output voltage. In order to improve the system efficiency, the flyback is operated in DCM, so that when the secondary-side current is zero, the quasi-resonance (QR) begins. According to the power expression. Then, the turns ratio of primary-side and secondary-side is set to be 36:8. The secondary-side inductor L_s of the transformer.

The capacitor C1 is calculated as (21), where ω_r is 5%~10% of the switching frequency f_s . So C1 is set to be 220nF.

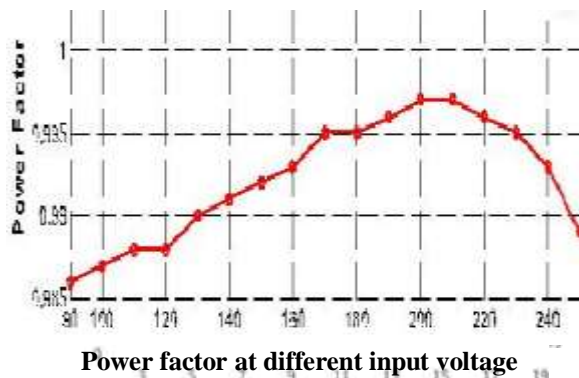
Here, Q is 7N60B, D6 and D7 are F8L60.

The input voltage and current are shown in Fig. 7. As observed, the input current follows the input voltage perfectly. When the PFC cell SEPIC circuit works in DCM, the PFC function can be achieved.



The PF and efficiency are shown in Fig. 8, when the input voltage changes from 90Vac to 260Vac. As shown in Fig. 8, the PF is always higher than 0.95 and the efficiency is also higher than 85%, with a maximum value of 90.8%. shows the PF and THD as the output power changes from 10% to 100%. The results satisfy the requirements of IEC61000-3-2. Input voltage, compared with the IEC61000-3-2 standard. The experimental results are lower than the corresponding standard limits.

To decrease the turn-on loss of the switch, QR method is adopted. As depicted, the turn-on voltage is relatively low to restrict the loss.



Input-current harmonics compared with IEC61000-3-2 class C standard.

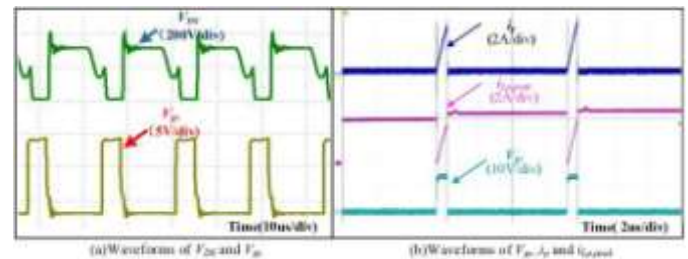
To decrease the turn-on loss of the switch, QR method is adopted. The driver signal and drain-source voltage, V_{ds} waveforms. As depicted, the turn-on voltage is relatively low to restrict the loss.

The peak current through the primary inductor L_p is detected by the proposed method shown in Fig. 11(b). As seen from Fig. 11(b), the detection point can be offset by the mirror capacitor.

t_{DIS} is also a main detection parameter, which includes the start and end instant detection. The start instant is the start time of secondary-side working time shown in Fig. 12 (a). The end instant is the start time of quasi-resonant period shown in Fig. 12 (b). Fig. 12 (a) shows how the integral capacitor can overcome the ambiguous vibrating voltage. Fig. 12 (b) demonstrates how a differential amplifier can rapidly show the interval end point better than a comparator because the hysteresis comparator still persists the time-delay. Therefore, it is demonstrated how through the presented scheme the detection of t_{DIS} is more accurate.

The current of ILED can be estimated by detecting the two main elements: $I_{Lp,peak}$ and t_{DIS} as mentioned in (15). Next, using the peak current control method, comparing the corresponding voltage V_{cs} of peak current. With corresponding V_{fb} of Iled, the turn OFF time can be obtained. The proposed estimator can reach a better accuracy than

reported.



Voltage and current signals during switching period

V. CONCLUSION

In this brief, an integrated-stage LED driver with primary-side-regulated characteristic is proposed. To better detect the start instant of the secondary-side working time t_{DIS} , an integrating capacitor is utilized. Moreover, a differential comparison method is proposed to capture the end instant of the secondary-side working time with high accuracy. In addition, to improve the precision of the sampled current, a novel sample-hold circuit has been developed. As a result, the power density and reliability of the system are improved by using primary-side-regulated method. The proposed methodologies have been experimentally verified by a 100W laboratory prototype, which showed high power factor, low input current distortion and an efficiency as high as 91%. In the future, with the increase of the working frequency of power MOSFETs, the primary-side-regulated method can further help to boost the power density of this kind of systems.

VI. REFERENCES

- [1] H.-A. Ahn, S.-K. Hong, and O.-K. Kwon, "A fast switching current regulator using slewing time reduction method for high dimming ratio of LED backlight drivers," *IEEE Trans. Circuits Syst. II, Exp. Briefs*, vol. 63, no. 11, pp. 1014–1018, Nov. 2016.
- [2] M. A. Pagliosa, R. G. Faust, T. B. Lazzarin, and I. Barbi, "Input-series and output-series connected modular single-switch flyback converter operating in the discontinuous conduction mode," *IET Power Electron.*, vol. 9, no. 9, pp. 1962–1970, Jul. 2016.
- [3] X. Wu, J. Yang, J. Zhang, and Z. Qian, "Variable on-time (VOT)- controlled critical conduction mode buck PFC converter for high-input AC/DC HB-LED lighting applications," *IEEE Trans. Power Electron.*, vol. 27, no. 11, pp. 4530–4539, Nov. 2012.
- [4] Y.-T. Hsieh, B. D. Liu, J. F. Wu, C. L. Fang, H. H. Tsai and Y. Z. Juang, "A high current accuracy boost white LED driver based on offset calibration technique," *IEEE Trans. Circuits Syst. II*,



Exp. Briefs, vol. 58, no. 4, pp. 244–248, Apr. 2011.

[4] Y. Wang, N. Qi, Y. Guan, C. Cecati, and D. Xu, “A single-stage LED driver based on SEPIC and LLC circuits,” *IEEE Trans. Ind. Electron.*, vol. 64, no. 7, pp. 5766–5776, Jul. 2017.

[5] Y. Wang, N. Qi, Y. Guan, C. Cecati, and D. Xu, “A single-stage LED driver based on SEPIC and LLC circuits,” *IEEE Trans. Ind. Electron.*, vol. 64, no. 7, pp. 5766–5776, Jul. 2017.

[6] P.-C. Hsieh, C.-J. Chang, and C.-L. Chen, “A primary-side-control quasi-resonant flyback converter with tight output voltage regulation and self-calibrated valley switching,” in *Proc. IEEE Energy Conv. Congr. Expo. (ECCE)*, Denver, CO, USA, 2013, pp. 3406–3412.

[7] P. Fang, Y.-F. Liu, and P. C. Sen, “A flicker-free single-stage offline LED driver with high power factor,” *IEEE Trans. Emerg. Sel. Topics Power Electron.*, vol. 3, no. 3, pp. 654–665, Sep. 2015